engineering proceedings

MDPI

Proceeding Paper

Investigation of the Influence of 3D-Printing Mode on the Accuracy of Geometric Shape †

Konstantin Chukalov [1,*], Sabi Sabev [1,2], Valeri Bakardzhiev [1,3], Plamen Kasabov [1,2], Agop Izmirliyan [1] and Georgi Hristozov [1]

[1] Department of Manufacturing Engineering and Technologies, Technical University Sofia, Plovdiv Branch, 25 Tsanko Dyustabanov Str., 4000 Plovdiv, Bulgaria; sabi_sabev@tu-plovdiv.bg (S.S.); bakardzhiev@tu-plovdiv.bg (V.B.); kasabov_p@tu-plovdiv.bg (P.K.); izmirliyan@tu-plovdiv.bg (A.I.); black8power@abv.bg (G.H.)
[2] Center of Competence "Smart Mechatronic, Eco- and Energy-Saving Systems and Technologies", 4000 Plovdiv, Bulgaria
[3] Department of Mechanics, Faculty of Mechanical Engineering, Technical University Sofia, Plovdiv Branch, 25 Tsanko Dyustabanov Str., 4000 Plovdiv, Bulgaria
* Correspondence: chukalov@tu-plovdiv.bg
† Presented at the International Conference on Electronics, Engineering Physics and Earth Science (EEPES2026), Bandirma, Turkey, 24–27 June 2026.

Abstract

In modern mechanical engineering, the requirements for surface roughness, geometric and dimensional accuracy are constantly increasing, as these characteristics are critical for the reliability, durability and functional application of products. The parameters of 3D printing significantly affect the quality, accuracy and physico-mechanical properties of the manufactured parts. This, in turn, necessitates a deeper understanding of the influence of printing modes on the accuracy and physico-mechanical properties of the printed component. The present study aims to determine the effect of the main technological parameters of the FFF process—printing speed and layer height—on the geometric accuracy and surface roughness of a functional machine element. For this purpose, a central composite design of experiments was developed to optimize both the process and the product. PETG was selected as the experimental material. The obtained results show that the layer height is the dominant factor influencing the roughness of the printed surface, while the printing speed exhibits a nonlinear effect within the considered range. The developed regression model allows determining an optimal range of printing parameters that achieves minimal surface roughness and high geometric accuracy of the part.

Keywords: 3D printing; surface roughness; dimensional accuracy

Check for updates

Academic Editors: Teodor Iliev, Ivaylo Stoyanov, Grigor Mihaylov and Selahattin Kosunalp

Published: 8 September 2026

Copyright: © 2026 by the authors. Licensee MDPI, Basel, Switzerland. This article is an open access article distributed under the terms and conditions of the Creative Commons Attribution (CC BY) license.

1. Introduction

3D printing is becoming a key technology in a number of industrial sectors such as medicine, mechanical engineering, pharmacy, architecture, aviation technologies, construction, biotechnology, food industry, and others [1–5]. Fused Filament Fabrication (FFF) is a 3D-printing process characterized by the use of a thermoplastic material—filament [6,7]. The technology involves the layer-by-layer deposition of a pre-created CAD model. FFF is one of the main technologies for additive manufacturing. Various materials are used, which can be recycled, emphasizing the environmental friendliness of the process. The most commonly used materials for 3D printing are PLA, PETG, and ABS, each characterized by different mechanical and thermal properties. In addition, advanced polymers such as PEEK,

polyetherimide and polyamide are increasingly used for high-performance engineering applications in aerospace, automotive and biomedical industries.

The proper operation of an assembled unit depends on the accuracy of its individual components. Various types of deviations from the geometric characteristics of a part exist, which are grouped into categories including linear and angular deviations, surface waviness and surface roughness [8–11]:

Dimensional accuracy and surface quality are among the most important indicators of engineering components. In engineering practice, surface roughness Ra is commonly used as the primary parameter for evaluating surface quality. Roughness affects the accuracy of assembly—in assembled units with small clearances, such as bushings, shafts, and rings, low roughness is required. If the roughness is too high, assembly becomes difficult and unstable. Low roughness of assembled units ensures greater durability due to reduced friction.

Reducer covers are structural elements that close the housing and support the proper operation of the gear drives and bearing assemblies. They perform mechanical, protective, and servicing functions by creating a closed, sealed environment for the lubrication of the mechanism. Additionally, they can accommodate bearing seats, sealing channels, and mounting elements, which makes them a key part of the overall reducer design.

The materials most commonly used under heavy loads are gray cast iron, aluminum, cast steel, and structural steels, with the choice depending on the application, thermal load, and required strength. Under light loads, plastic covers are increasingly being used. Due to the complex design features—the presence of ribs, channels, and flanges—3D-printed reducer covers are being increasingly employed. The tightness, operational reliability, and durability of the reducer depend on the quality of the contact surfaces, roughness, and dimensional accuracy of the manufactured part.

Numerous scientific studies have investigated the influence of FDM printing parameters on the quality of printed surfaces, including surface roughness and dimensional accuracy. Mushtaq et al. reported that layer thickness and printing speed significantly influence the surface roughness of PETG specimens, achieving a minimum roughness value of Ra = 6.8 μm under optimized conditions [12]. Shabeeb et al. also reported that layer height represents the dominant factor affecting the tensile strength and surface roughness of PETG printed parts [13]. In their recent study, Thotakuri et al. confirmed that layer thickness, infill density and printing speed have the most significant influence on the mechanical properties, dimensional accuracy and surface quality of PETG components manufactured using FFF technology [14]. The authors also noted that the majority of published studies are primarily focused on the optimization of standardized specimens and indicators related to the sustainability of the manufacturing process. In summary, these studies demonstrate that FDM process parameters significantly affect the dimensional accuracy, surface quality and mechanical performance of PETG printed components.

Despite the considerable number of studies dedicated to the optimization of FDM process parameters, limited attention has been paid to functional engineering components containing assembly-critical geometrical features such as bearing seats, sealing surfaces and contact regions with increased requirements for dimensional accuracy and surface quality. Unlike the standardized benchmark specimens commonly used in previous investigations, reducer covers contain functionally significant surfaces that directly affect assembly accuracy, sealing capability and the operational reliability of the mechanical system.

The present study addresses these limitations by investigating the geometry of a functional mechanical component—a reducer cover manufactured from PETG material using FFF technology. As a result, an assessment of both surface roughness and dimensional

deviations in the critical functional surfaces was carried out through the application of experimental design and regression modeling.

The reviewed studies primarily report R^2 values and *p*-values without explicitly evaluating lack-of-fit [14–18]. Consequently, the adequacy of the developed regression models for describing the systematic process behavior remains insufficiently validated. A significant lack-of-fit would indicate that additional factors beyond printing speed and layer height are needed—an issue that has not been addressed in the PETG literature.

The objective of the present study is to determine the influence of the main FFF process parameters, namely printing speed and layer height, on the dimensional accuracy and surface roughness of functionally critical surfaces of a PETG reducer cover.

2. Materials and Methods

PETG filament was selected as the experimental material due to its widespread use as a technical material for printing components with various functional applications. This is primarily attributed to its good dimensional stability, low warping tendency, high impact resistance and suitability for functional engineering applications. The main mechanical properties of the material provided by the manufacturer are presented in Table 1.

Table 1. Mechanical properties of PETG.

Properties	Units	ASTM Test	PETG
Tensile strength	Psi	D638	7700
Tensile modulus of elasticity	Psi	D638	320,000
Tensile elongation	%	D638	210
Flexural strength	Psi	D790	11,200
Flexural modulus of elasticity	Psi	D790	310,000

The investigated component (shown in Figure 1) represents a functional reducer cover whose design contains several features of critical importance for its assembly capability and manufacturability. Unlike the standardized benchmark specimens commonly used in previous studies, the selected specimen contains real geometrical features through which contact or assembly with other components of the mechanical assembly is achieved. The geometrical accuracy and surface quality of these printed features directly affect their operational performance and functional suitability.

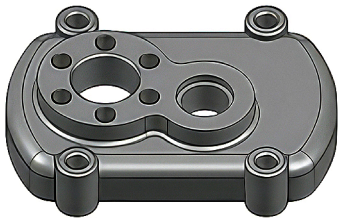


Figure 1. Isometric view of the model.

For the fabrication of the test samples shown in Figure 1, an "Ender 3 V2 Pro" 3D printer, model 3v2-Pro with 0.4 brass nozzle, was used. The printing process was controlled using Cura slicing software v.5.13. The selected experimental parameters, such as the nozzle and bed temperatures, printing speed, and layer height of the FDM 3D printer, were chosen based on the recommended values of the material manufacturer as well as the machine parameters (Table 2).

Table 2. Printing parameters.

Printing Parameters	Values
FDM 3D printer nozzle temperature	235 °C
FDM 3D printer heated bed temperature	75 °C
First layer printing speed	15 mm/s
Model infill	100% density
Initial layer infill speed	20 mm/s
Inner wall printing speed	60 mm/s

A central composite design (CCD) was applied to investigate the influence of printing speed and layer height on the selected response parameters. The experimental design included factorial points, axial points and five center points used for estimation of the experimental error and evaluation of model adequacy through lack-of-fit analysis. In order to improve the statistical reliability of the experimental results, all experimental runs from the initial 13-point CCD matrix were repeated three times.

Both linear and quadratic regression models were developed using Minitab 17 software. The quadratic approximation was introduced in order to improve the predictive capability and adequacy of the regression analysis. Prior to regression modeling, coded factor centering was applied to improve the numerical stability of the developed models and reduce parameter correlation. The adequacy of the regression models was evaluated using analysis of variance (ANOVA), coefficients of determination (R^2, adjusted R^2 and predicted R^2), residual analysis and lack-of-fit testing. Particular attention was paid to the adequacy of the developed regression models and to the interpretation of statistically significant lack-of-fit results.

For each sample, a printing program was created based on the calculated values of the two variable factors shown in Table 3.

Table 3. Central composite design of experiments and factor levels.

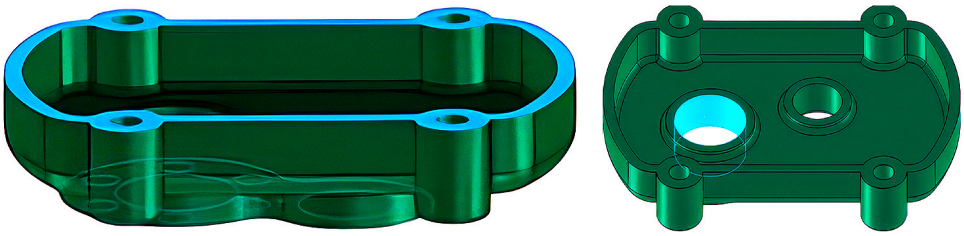
Sample	Factor A Levels	Factor B Levels	Factor Value Speed (mm/s)	Factor Value Height (mm)
1	0.00	0.00	45.00	0.23
2	1.00	−1.00	60.00	0.15
3	0.00	0.00	45.00	0.23
4	0.00	1.41	45.00	0.33
5	0.00	0.00	45.00	0.23
6	0.00	0.00	45.00	0.23
7	1.41	0.00	66.15	0.23
8	−1.41	0.00	23.85	0.23
9	0.00	−1.41	45.00	0.11
10	0.00	0.00	45.00	0.23
11	−1.00	−1.00	30.00	0.15
12	−1.00	1.00	30.00	0.30
13	1.00	1.00	60.00	0.30

To represent the stochastic relationship between the investigated parameters and the factors that determine them, linear models (first-order) and nonlinear models (second-order or higher) are applied. In cases where the nature of the model is not known from prior information, a hypothesis is made that it is linear. In such a model, the variable factors participate only at the first degree.

For roughness measurement, a mobile roughness tester with a resolution of 0.001 µm was used. A 3D coordinate measuring machine with measurement accuracy of 0.003 mm (3 µm) along the X, Y, and Z axes was employed for the study.

Depending on the influence of the accuracy of a given dimension on the motion, operation, or assembly of a mechanical engineering product, two groups are classified: functional dimensions and non-functional dimensions. A functional dimension for the reducer cover is the distance between the two walls, because it affects the axial position of the shafts, the seals, and the reliability of the entire reducer. For the purposes of this paper, a linear dimension along the *Y*-axis between walls A and B was selected.

The classification of form deviations is analogous. Functional form deviations represent the differences between the actual geometric characteristics of the part and the ideal shapes specified in the drawing. They indicate the extent to which the manufactured element deviates from the exact geometry required for proper functioning. Functional form deviations in mechanical engineering are those related to guiding surfaces, bearing holes, shaft cylindricity, concentricity of bearings and bearing supports, axis positions, etc. For the specific part, the following functional form deviations were selected: linear dimensional deviation between the two base surfaces shown in Figure 2a, and deviation from the nominal hole diameter of the bearing mounting hole shown in Figure 2b.



(**a**) (**b**)

Figure 2. Measured surfaces of the part: (**a**) flat surface; (**b**) hole surface.

The roughness of assembly surfaces directly affects the accuracy, friction, wear, sealing, and stability of the joint. For roughness measurement, the connecting surface of the model and the main hole in which the bearing for the reducer shaft is mounted were selected. Surface roughness measurements were performed using a portable HUATEC SRT-6210(Beijing, China) roughness tester equipped with an inductive probe and a diamond stylus tip shown in Figure 3. The device enables measurement of the roughness parameters Ra, Rz, Rq and Rt in accordance with ISO standards. The measuring range for the Ra parameter is 0.005–16 µm, with a resolution of 0.001 µm for values below 10 µm. The measurements were carried out on the functional contact surfaces and bearing mounting regions of the reducer cover in order to evaluate the influence of the selected FFF process parameters on the surface quality of the printed component.



Figure 3. HUATEC SRT-6210 roughness tester.

3. Results

The results of the conducted experiment demonstrate that, just as the machining of metal workpieces by milling and turning is subject to quality control, so is the printing of models and specimens from polymers and plastics. After comparing the obtained results,

the specimen with parameters closest to the designed model was selected, which will serve as a template for the production of parts based on the designed model.

3.1. Dimensional Accuracy of Functional Features

The linear dimension deviation aims to provide the actual deviations when printing with different modes, and the results of the deviations are shown in Table 4.

Table 4. Measured linear dimension of the specimens.

# Test Sample	Nominal Value (mm)	Dimensional Deviation (mm)
TS-00	60.000	-
TS-01	60.018	0.018
TS-02	60.054	0.054
TS-03	60.025	0.025
TS-04	60.020	0.02
TS-05	60.009	0.009
TS-06	60.017	0.017
TS-07	60.053	0.053
TS-08	60.008	0.008
TS-09	60.016	0.016
TS-10	60.009	0.009
TS-11	60.015	0.015
TS-12	60.017	0.017
TS-13	59.995	0.008

For the 13 specimens, the distance between the two parallel outer walls was measured. This dimension represents a functional parameter affecting the positioning and sealing of the cover relative to the gearbox housing. Deviations from the nominal value (60.00 mm) are presented in Table 4. The smallest deviation (0.008 mm) was observed for specimens TS-08 and TS-13, while the largest deviation (0.054 mm) was observed for TS-02. According to the dimensional tolerance classes defined in ISO 286 [19], the results obtained for specimens TS-05, TS-08, TS-10, and TS-13 correspond to IT5 accuracy grade. Compared to conventional machining processes for a similar type of component, this level of accuracy would correspond to fine milling [15,20].

The overall dimensional variation range for the investigated interval of printing speed and layer height was 0.053 mm. According to the standard, this corresponds to IT8–IT9 accuracy grade, which is comparable to a conventional finish milling operation.

The investigated 60 mm dimension corresponds to the overall size of the gearbox cover. In industrial practice, such surfaces are often produced directly by the process used for manufacturing the blank, most commonly casting. Comparing the obtained printing results with the technological capabilities of casting processes, it can be concluded that the achieved accuracy is significantly higher than that of gray cast iron sand casting, which typically achieves IT13–IT16 accuracy grades. The obtained accuracy is comparable to aluminum permanent mold casting processes achieving IT9–IT11 accuracy grades, and also comparable to precision die casting processes capable of achieving IT7–IT9 accuracy grades [20,21].

During the measurements of the printed specimens, the diameter of the hole in which the bearing for the central shaft of the reducer will be mounted was also measured. The results are compared with those of the designed model, with the closest results providing information on the optimal printing mode. The measurement results are presented in Table 5. The designed model is designated as TS-00, and the printed models as TS-01 to TS-13, respectively.

Table 5. Measured diameter of the bearing seat hole for the tested specimens.

# Test Sample	Nominal Value (mm)	Dimensional Deviation (mm)
TS-00	20.000	-
TS-01	19.798	0.202
TS-02	19.736	0.264
TS-03	19.883	0.117
TS-04	19.763	0.237
TS-05	19.821	0.179
TS-06	19.746	0.254
TS-07	19.829	0.171
TS-08	19.692	0.308
TS-09	19.739	0.261
TS-10	19.783	0.217
TS-11	19.780	0.220
TS-12	19.826	0.174
TS-13	19.838	0.162

After systematizing the results, it was observed that the smallest deviation was achieved in experiment TS-03, where a deviation of 0.117 mm was obtained. The largest dimensional deviation was recorded in experiment TS-08, where a deviation of 0.308 mm was measured. To a certain extent, this result was expected due to the central positioning of the hole within the cover and the effect of shrinkage during the cooling of the component. According to SKF recommendations, bearing mounting surfaces require significantly higher dimensional accuracy and surface quality than those obtained directly after FFF printing [22].

According to ISO 286 [19], the obtained minimum deviation corresponds approximately to IT10–IT11 accuracy grade. Considering the functional purpose of the surface defined by this dimension, namely a bearing seat, the required tolerance should be within the IT6–IT7 range according to the bearing tolerance standard ISO 492 [23]. This clearly indicates that the bearing seat produced by the 3D-printing process requires subsequent finishing machining and should rather be considered as a blank or semi-finished part.

Compared to other methods for producing blanks, such as casting, the achieved accuracy can be considered comparable to sand casting and permanent mold casting processes.

3.2. Surface Roughness of Functional Features

In order to obtain information on which type of seal to use or for subsequent post-processing of the model, measurements were conducted to determine the roughness of all test specimens. The measurements provide information on the optimal printing mode that yields results closest to those of the designed model. The results are obtained in Table 6.

The roughness results associated with the planar surface of the cover, intended for assembly with the gearbox housing, are within the range of 3.98 μm to 12.24 μm. In this case, the investigated surface was in contact with the printer build plate during the printing process, which leads to the presence of inherited roughness caused by the replication of the build plate microtexture onto the first printed layer.

The obtained roughness is largely dependent on the conditions under which the first layer is formed. At lower printing speeds, the extruded material has more time to spread and conform to the texture of the build plate, resulting in improved adhesion and a more homogeneous surface. A significant influence is also exerted by the calibration of the nozzle height, since it determines the degree of compression, 'squish' of the first layer and consequently the actual contact area with the build plate.

Table 6. Surface roughness (Ra) of the reducer cover contact surface.

# Test Sample	Surface Roughness Ra (μm)
TS-01	6.19
TS-02	5.77
TS-03	4.39
TS-04	12.24
TS-05	9.00
TS-06	5.08
TS-07	6.05
TS-08	4.35
TS-09	5.73
TS-10	7.43
TS-11	5.49
TS-12	3.98
TS-13	7.11

In the present case, the layer height has a smaller effect on the resulting roughness. Its influence is mainly related to the pressure exerted by the nozzle and the subsequent layers onto the first layer during the fabrication of the part.

The values summarized in the results indicate a high level of roughness of the investigated contact surface. This once again reinforces the hypothesis that, for the manufacturing of functional machine elements, 3D printing based on FFF technology should rather be used for the production of blanks or semi-finished parts that require additional machining prior to assembly (Table 7).

Table 7. Surface roughness (Ra) of the bearing mounting hole.

# Test Sample	Surface Roughness Ra (μm)
TS-01	20.30
TS-02	15.57
TS-03	20.92
TS-04	30.35
TS-05	17.71
TS-06	20.08
TS-07	23.20
TS-08	24.59
TS-09	13.39
TS-10	21.23
TS-11	15.28
TS-12	24.05
TS-13	27.09

To determine the optimal printing mode and the applicability of the printed models, in addition to measuring the roughness of the connecting surface for mounting the model—the reducer cover—to the reducer housing, roughness measurements were also performed on the hole for mounting the bearing of the main shaft of the reducer. To ensure a tight fit of the bearing in the hole, the roughness of the hole wall was measured for each model. After conducting the roughness measurements, the obtained results were compared with those of the designed model, again designated as TS-00.

As expected, the roughness measurements of the cylindrical surfaces of the bearing seats along the vertical direction, which coincides with the printing *Z*-axis, show significantly higher values. In this case, the layer height has a greater influence, as it forms printed

layers with different elliptical cross-sections, while the printing speed has a significant effect on the staircase effect.

Based on the obtained results, it can be concluded that none of the investigated printing regimes are capable of producing a printed surface roughness that satisfies the roughness requirements for bearing seats (0.8–1.6 μm) [20].

3.3. Regression Analysis of Surface Roughness Results

A linear regression model presented in Equation (1) fitted to the initial 13 runs (without replication) explained only 58.11% of the variation (R^2 = 58.11%) and showed a significant lack-of-fit (p = 0.024).

$$R_a = 4.96 + 0.01034V_p + 54.8H_p \ \ (\mu m) \quad (1)$$

To improve statistical reliability, each factor combination was repeated three times, giving a total of 39 specimens. The linear model presented in Equation (2) based on the replicated data achieved R^2 = 79.82%, but the lack-of-fit test remained significant (p = 0.001). This clearly indicates that a linear approximation is insufficient and that a quadratic model is required.

$$R_a = 4.41 + 0.0105V_p + 72.11H_p \ \ (\mu m) \quad (2)$$

Because the uncoded quadratic model exhibited high multicollinearity (VIF values up to 60), the factor levels were centered. The final quadratic regression model in terms of centered variables (A—printing speed, B—layer height) is:

$$R_a = 20.047 + 0.157A + 5.52B + 1.321A^2 + 0.307B^2 + 0.657AB \ \ (\mu m) \quad (3)$$

A quadratic regression model describing the relationship between the process parameters and the resulting surface roughness was developed using centered variables. The obtained regression equation is presented in Equation (3) and expresses the surface roughness Ra as a function of the investigated factors and their quadratic and interaction terms.

The summary statistics of the developed quadratic regression model are presented in Table 8. The coefficient of determination reaches R^2 = 84.64%, indicating that the model explains a substantial portion of the variability of the response variable. The adjusted coefficient of determination, R^2(adj) = 82.31%, confirms that the explanatory capability of the model remains high after accounting for the number of predictors. In addition, the predicted coefficient of determination R^2(pred) = 77.92% indicates good predictive performance of the model. The relatively low value of the residual standard deviation S = 2.06272 further confirms the adequacy of the developed regression model for describing the relationship between the process parameters and the resulting surface roughness.

Table 8. Summary statistics of the quadratic regression model for surface roughness.

S	R-sq	R-sq (Adj)	R-sq (Pred)
2.06272	84.64%	82.31%	77.92%

The estimated regression coefficients of the quadratic model are presented in Table 9. The statistical analysis indicates that the layer height (B) has a highly significant effect on surface roughness $p < 0.001$, while the linear effect of printing speed (A) is statistically insignificant p = 0.712. The quadratic term A^2 is statistically significant p = 0.006, indicating a nonlinear influence of printing speed on the surface roughness. In contrast, the quadratic term B^2 and the interaction term A × B are not statistically significant at the 95% confi-

dence level. The variance inflation factor (VIF) values close to 1 indicate the absence of multicollinearity between the model terms.

Table 9. Regression coefficients of the quadratic model for surface roughness.

Term	Coef	SE Coef	T-Value	*p*-Value	VIF
Constant	20.047	0.533	37.64	0.000	
A	0.157	0.421	0.37	0.712	1.00
B	5.520	0.421	13.11	0.000	1.00
A × A	1.321	0.452	2.92	0.006	1.02
B × B	0.307	0.452	0.68	0.501	1.02
A × B	0.657	0.595	1.10	0.278	1.00

The results of the analysis of variance (ANOVA) for the quadratic regression model are presented in Table 10. The regression model is statistically significant, as indicated by the high F-value (36.37) and the corresponding p-value < 0.001, confirming that the model adequately describes the relationship between the investigated factors and surface roughness. The analysis shows that layer height (B) has a dominant and statistically significant effect on the response F = 171.86, $p < 0.001$, while the linear effect of printing speed (A) is not statistically significant. The quadratic term (A^2) is statistically significant $p = 0.006$, indicating a nonlinear influence of printing speed on surface roughness. In contrast, the quadratic term B^2 and the interaction term (A × B) are not statistically significant at the 95% confidence level. The "lack-of-fit" test $p = 0.004$ suggests that although the quadratic model explains a substantial portion of the variability of the response, some systematic variation remains not fully captured by the model.

Table 10. Analysis of variance (ANOVA) for the quadratic regression model of surface roughness.

Source	DF	Adj SS	Adj MS	F-Value	*p*-Value
Regression	5	773.776	154.755	36.37	0.000
A	1	0.588	0.588	0.14	0.712
B	1	731.236	731.236	171.86	0.000
A × A	1	36.391	36.391	8.55	0.006
B × B	1	1.969	1.969	0.46	0.501
A × B	1	5.175	5.175	1.22	0.278
Error	33	140.409	4.255		
Lack-of-Fit	3	50.337	16.779	5.59	0.004
Pure Error	30	90.072	3.002		
Total	38	914.185			

At low speeds, the extruded material exhibits better adhesion and forms a smoother surface, but excessively low speeds increase cooling time and the risk of local overheating. At high speeds, conversely, cooling is insufficient and thermoplastic deformation of the strands occurs, which increases roughness Ra. Layer height has a consistently positive influence—as it increases, the geometric step between layers grows and the micro-geometric unevenness increases. It follows that to achieve minimal roughness, the smallest possible layer height should be used at a medium to high printing speed that does not compromise the thermal balance of the process. Based on the experimental range and the derived equation, the following practical guidelines can be formulated: Optimal printing speed: approximately 45–50 mm/s—in this zone, Ra reaches minimum values before the onset of thermal saturation. Optimal layer height: 0.10–0.12 mm, which ensures the smoothest surface and stable process. Under these conditions, the predicted roughness value calculated by the model is approximately Ra ≈ 15–17 μm.

The recommended range for the reducer cover depends on the type of seal. When using an elastic gasket (O-ring or rubber strip), the obtained results are acceptable because the material deforms and the seal compensates for surface irregularities. The combination of a plastic cover and a metallic seal is very rarely used in engineering practice, because the metallic seal can scratch or deform the plastic cover, which may impair the joint behavior. Metals and plastics also have different thermal expansion, making such a joint impractical. For metallic seals, the recommended roughness is 5–10 μm, which necessitates additional post-processing of the plastic cover.

4. Conclusions

The obtained results demonstrate that the dimensional accuracy and surface quality of functional PETG reducer covers manufactured by FFF technology strongly depend on the selected process parameters and the geometry of the investigated functional surfaces.

For the purposes of the study, a real engineering component—a gearbox cover—was used. Its design incorporates several critical surfaces, such as the contact surface with the gearbox housing, bearing seats, and other functional features directly affecting the manufacturability of the assembly process and the quality of the assembled component. This represents one of the major differences compared to many previous studies on the investigated material, where simplified test specimens with less complex geometry were used. Consequently, this approach makes it possible to evaluate the practical influence of the combination of varying manufacturing parameters and the geometric complexity of the investigated part.

In the present study, a methodology for the evaluation and control of the surface roughness of a functional surface, namely the wall of the bearing seat of a gearbox cover, is proposed through the development of regression models. The methodology is based on a standard design of experiments comprising 13 experimental points and 5 repetitions at the center point.

The initially developed regression model demonstrated limited predictive capability and insufficient accuracy in describing the observed variations in the investigated process. This necessitated the implementation of a second stage of the study, involving a threefold replication of the experimental matrix. As a result, an improvement in the descriptive and predictive capability of the new regression model was observed.

For the purpose of a more in-depth analysis of the process, the lack-of-fit criterion was also applied, enabling an assessment of the adequacy of the employed model and the selected input parameters. It should be noted that this criterion represents a powerful tool for evaluating the quality of statistical models; however, its application remains relatively limited in similar studies within the field.

The obtained results indicate a statistically significant lack-of-fit, suggesting the presence of unexplained relationships between the investigated variables or the influence of factors not included in the model. In order to examine the existence of higher-order nonlinear relationships, a quadratic regression model was additionally developed.

The results obtained from the quadratic model demonstrate a certain improvement in the values of the lack-of-fit criterion; however, it remains statistically significant. This indicates the necessity for further investigations involving additional technological parameters and factors influencing the 3D printing process. Similar observations regarding shrinkage effects, thermal instability and geometry-dependent printing defects have also been reported in recent investigations focused on optimization and thermal behavior of FFF-printed polymer components with complex geometries [24,25].

Based on the obtained experimental results, practical recommendations for the selection of operating parameters for 3D printing of similar PETG components can be formu-

lated. The optimal operating parameters within the investigated range are printing speed of 45–50 mm/s and layer height of 0.10–0.12 mm.

The investigation of additional printing parameters, such as extruder temperature, infill percentage, and part orientation, represents an important direction for future research. The results of these future investigations are expected to provide a better understanding of the lack-of-fit values obtained in the present study. Further scientific interest also lies in investigating the mechanical properties and load-bearing capacity of 3D-printed gearbox components.

Author Contributions: Conceptualization, K.C. and P.K.; methodology, K.C., S.S. and P.K.; software G.H.; validation, K.C., A.I. and V.B.; formal analysis, K.C. and P.K.; investigation, K.C. and V.B.; resources, G.H.; data curation, A.I. and P.K.; writing—original draft preparation, K.C., G.H. and P.K.; writing—review and editing, A.I. and K.C.; visualization, A.I. and P.K.; supervision, K.C. and V.B.; project administration, K.C., S.S. and V.B.; funding acquisition, S.S. and P.K. All authors have read and agreed to the published version of the manuscript.

Funding: This research was funded by the European Regional Development Fund within the OP "Research, Innovation and Digitalization Programme for Intelligent Transformation 2021–2027", Project № BG16RFPR002-1.014-0005 Center of competence "Smart Mechatronics, Eco- and Energy Saving Systems and Technologies".

Institutional Review Board Statement: Not applicable.

Informed Consent Statement: Not applicable.

Data Availability Statement: Data will be available on request.

Conflicts of Interest: The authors declare no conflicts of interest.

Abbreviations

The following abbreviations are used in this manuscript:

FFF	Fused Filament Fabrication
CAD	Computer-Aided Design
PLA	Polylactic Acid
PETG	Polyethylene Terephthalate Glycol
ABS	Acrylonitrile Butadiene Styrene
PEEK	Polyether Ether Ketone
ANOVA	Analysis of Variance
AICc	Corrected Akaike Information Criterion
BIC	Bayesian Information Criterion

References

1. Li, J.; Wu, C.; Chu, P.K.; Gelinsky, M. 3D printing of hydrogels: Rational design strategies and emerging biomedical applications. *Mater. Sci. Eng. R Rep.* **2020**, *140*, 100543. [CrossRef]
2. Rastin, H.; Ormsby, R.T.; Atkins, G.J.; Losic, D. 3D Bioprinting of Methylcellulose/Gelatin-Methacryloyl (MC/GelMA) Bioink with High Shape Integrity. *ACS Appl. Bio Mater.* **2020**, *3*, 1815–1826. [CrossRef] [PubMed]
3. Jamróz, W.; Szafraniec, J.; Kurek, M.; Jachowicz, R. 3D Printing in Pharmaceutical and Medical Applications—Recent Achievements and Challenges. *Pharm. Res.* **2018**, *35*, 176. [CrossRef] [PubMed]
4. Xu, W.; Wang, X.; Sandler, N.; Willför, S.; Xu, C. Three-Dimensional Printing of Wood-Derived Biopolymers: A Review Focused on Biomedical Applications. *ACS Sustain. Chem. Eng.* **2018**, *6*, 5663–5680. [CrossRef] [PubMed]
5. Buj-Corral, I.; Tejo-Otero, A.; Fenollosa-Artés, F. Development of am technologies for metals in the sector of medical implants. *Metals* **2020**, *10*, 686. [CrossRef]
6. Solomon, I.; Sevvel, P.; Gunasekaran, J. A Review on the Various Processing Parameters in FDM. *Mater. Today Proc.* **2021**, *37*, 509–514. [CrossRef]

7. Equbal, A.; Murmu, R.; Kumar, V. Advancements in Dimensional Accuracy in Fused Deposition Modeling. *AIMS Mater. Sci.* **2024**, *11*, 950–990. [CrossRef]
8. Carolo, L.C.B.; Cooper, R.E.O. A Review on the Influence of Process Variables on the Surface Roughness of Ti-6Al-4V by Electron Beam Powder Bed Fusion. *Addit. Manuf.* **2022**, *59*, 103103. [CrossRef]
9. Karamanli, I.; Tahnal, K. Optimization of Printing Parameters of PLA and ABS Produced by FFF. *J. Mater. Mechatron. A* **2024**, *5*, 286–302. [CrossRef]
10. Górski, F.; Kuczko, W.; Wichniarek, R. Influence of Process Parameters on Dimensional Accuracy of Parts Manufactured Using Fused Deposition Modelling Technology. *Adv. Sci. Technol. Res.* **2013**, *7*, 27–35. [CrossRef]
11. Alexopoulou, V.E.; Christodoulou, I.T.; Markopoulos, A.P. Effect of Printing Speed and Layer Height on Geometrical Accuracy of FDM-Printed Resolution Holes of PETG Artifacts. *Eng. Proc.* **2022**, *24*, 11. [CrossRef]
12. Arreda, N.; Isksioui, H.; Boutahri, H.; L'kadiba, A.; Elmoussami, H. FDM Process Parameters Impact on Roughness and Dimensional Accuracy of PLA Parts. *Eng. Proc.* **2025**, *112*, 6. [CrossRef]
13. Mushtaq, R.T.; Iqbal, A.; Wang, Y.; Khan, A.M.; Abu Bakar, M.S. Parametric Optimization of 3D Printing Process Hybridized with Laser-Polished PETG Polymer. *Polym. Test.* **2023**, *125*, 108129. [CrossRef]
14. Abdulridha, H.H.; Obaeed, N.H.; Jaber, A.S. Optimization of Fused Deposition Modeling Parameters for Polyethylene Terephthalate Glycol Flexural Strength and Dimensional Accuracy. *Adv. Sci. Technol. Res. J.* **2025**, *19*, 50–64. [CrossRef] [PubMed]
15. Shabeeb, A.H.; Abdulwahhab, A.B.; Ismael, H.S.; Ghazi, S.K. Optimization of Fused Deposition Modeling Parameters to Enhance Tensile Strength and Surface Roughness of Polyethylene Terephthalate Glycol. *Adv. Sci. Technol. Res. J.* **2025**, *19*, 345–358. [CrossRef] [PubMed]
16. Thotakuri, M.; Yelamasetti, B.; Sri Phani, I.S.; Shareef Sk, M.; Kumar, P.N. Process Parameter Optimization of Fused Filament Fabrication—3D Printing with PETG: A Multi-Objective Approach Using the Matrix Method. *Rapid Prototyp. J.* **2026**, *32*, 799–820. [CrossRef]
17. Almansoori, K.; Pervaiz, S. Effect of Layer Height, Print Speed and Cell Geometry on Mechanical Properties of Marble PLA Based 3D Printed Parts. *Results Eng.* **2023**, *1*, 100023. [CrossRef]
18. Frunzaverde, D.; Cojocaru, V.; Bacescu, N.; Ciubotariu, C.-R.; Miclosina, C.-O.; Turiac, R.R.; Marginean, G. The Influence of the Layer Height and the Filament Color on the Dimensional Accuracy and the Tensile Strength of FDM-Printed PLA Specimens. *Polymers* **2023**, *15*, 2377. [CrossRef] [PubMed]
19. *Standard No. ISO 286-1:2010*; Geometrical Product Specifications (GPS)—ISO Code System for Tolerances on Linear Sizes—Part 1: Basis of Tolerances, Deviations and Fits. ISO: Geneva, Switzerland, 2010.
20. Oberg, E.; Jones, F.D.; Horton, H.L.; Ryffel, H.H. *Machinery's Handbook*, 32nd ed.; Industrial Press: New York, NY, USA, 2024.
21. *Standard No. ISO 8062-3:2007*; Geometrical Product Specifications (GPS)—Dimensional and Geometrical Tolerances and Machining Allowances for Castings—Part 3: General Dimensional and Geometrical Tolerances and Machining Allowances for Castings. ISO: Geneva, Switzerland, 2007.
22. SKF. Accuracy of Seats and Abutments. Available online: https://www.skf.com/id/products/super-precision-bearings/principles/bearing-selection-process/bearing-interfaces/accuracy-of-seats (accessed on 20 May 2026).
23. *Standard No. ISO 492:2014*; Rolling Bearings—Radial Bearings—Geometrical Product Specifications (GPS) and Tolerance Values. ISO: Geneva, Switzerland, 2014.
24. Bankov, B.; Todorov, T.T.; Todorov, G. A Functional Model Printing Approach Optimized for Cost-Efficiency Using FDM Technology. *Eng. Proc.* **2025**, *100*, 53. [CrossRef]
25. Paneva, M.; Panev, P. An Approach for the Accelerated Heat Aging of Test Specimens Produced Using 3D Additive Materials. *Eng. Proc.* **2025**, *100*, 47. [CrossRef]

Disclaimer/Publisher's Note: The statements, opinions and data contained in all publications are solely those of the individual author(s) and contributor(s) and not of MDPI and/or the editor(s). MDPI and/or the editor(s) disclaim responsibility for any injury to people or property resulting from any ideas, methods, instructions or products referred to in the content.